

# UC Davis

## UC Davis Previously Published Works

### Title

Computer-Aided Selective Optimization of Side Activities of Talinolol

### Permalink

<https://escholarship.org/uc/item/2tb1g3vf>

### Journal

ACS Medicinal Chemistry Letters, 10(6)

### ISSN

1948-5875

### Authors

Hiesinger, Kerstin

Kramer, Jan S

Achenbach, Janosch

et al.

### Publication Date

2019-06-13

### DOI

10.1021/acsmchemlett.9b00075

Peer reviewed

# Computer-Aided Selective Optimization of Side Activities of Talinolol

Kerstin Hiesinger,<sup>†,∇</sup> Jan S. Kramer,<sup>†,∇</sup> Janosch Achenbach,<sup>†</sup> Daniel Moser,<sup>†</sup> Julia Weber,<sup>†</sup> Sandra K. Wittmann,<sup>†</sup> Christophe Morisseau,<sup>‡</sup> Carlo Angioni,<sup>§</sup> Gerd Geisslinger,<sup>§,||</sup> Astrid S. Kahnt,<sup>†</sup> Astrid Kaiser,<sup>†</sup> Anna Proschak,<sup>†</sup> Dieter Steinhilber,<sup>†,||</sup> Denys Pogoryelov,<sup>⊥</sup> Karen Wagner,<sup>‡</sup> Bruce D. Hammock,<sup>‡,Ⓢ</sup> and Ewgenij Proschak<sup>\*,†,||,Ⓢ</sup>

<sup>†</sup>Institute of Pharmaceutical Chemistry, Goethe-University of Frankfurt, Max-von-Laue Strasse 9, D-60438 Frankfurt am Main, Germany

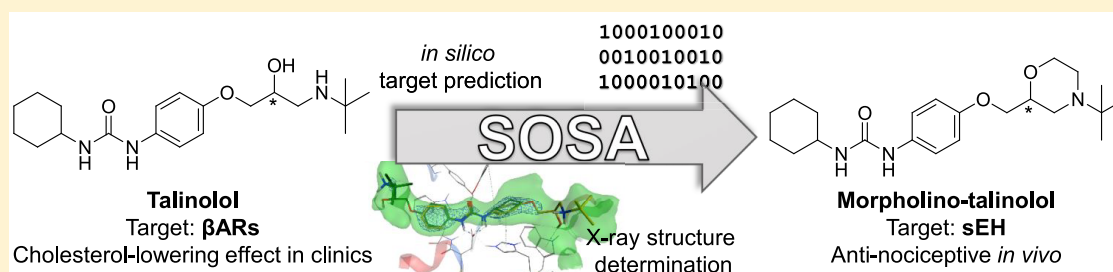
<sup>‡</sup>Department of Entomology and Nematology and UC Davis Comprehensive Cancer Center, University of California Davis, One Shields Avenue, Davis, California 95616, United States

<sup>§</sup>Institute of Clinical Pharmacology, Pharmazentrum Frankfurt, ZAFES, Theodor-Stern-Kai 7, D-60590 Frankfurt am Main, Germany

<sup>||</sup>Branch for Translational Medicine and Pharmacology, Fraunhofer Institute for Molecular Biology and Applied Ecology IME, Theodor-Stern-Kai 7, D-60590 Frankfurt am Main, Germany

<sup>⊥</sup>Institute of Biochemistry, Goethe-University of Frankfurt, Max-von-Laue Strasse 9, D-60438 Frankfurt am Main, Germany

## Supporting Information



**ABSTRACT:** Selective optimization of side activities is a valuable source of novel lead structures in drug discovery. In this study, a computer-aided approach was used to deorphanize the pleiotropic cholesterol-lowering effects of the beta-blocker talinolol, which result from the inhibition of the enzyme soluble epoxide hydrolase (sEH). X-ray structure analysis of the sEH in complex with talinolol enables a straightforward optimization of inhibitory potency. The resulting lead structure exhibited *in vivo* activity in a rat model of diabetic neuropathic pain.

**KEYWORDS:** Selective optimization of side activities, soluble epoxide hydrolase, polypharmacology, computer-aided drug design, structure-based drug design

Selective optimization of side activities, also known as the SOSA approach, has been proposed to be a very effective method of lead identification and optimization.<sup>1</sup> Following SOSA, a side activity of a drug, which is observed in clinics, is enhanced by subsequent introduction of structural changes. SOSA is an extremely promising strategy to identify novel lead structures exhibiting good bioavailability and low toxicity due to the fact that the starting point has been already approved in humans. However, in most cases the side activity of a drug is an adverse effect or quite weak and is only reported from clinical trials or clinical practice.

Talinolol (**1**) is an unselective antagonist of the beta adrenergic receptors ( $\beta$ AR), also referred to as a beta-blocker, and is used as an antihypertensive agent. Interestingly, in several small clinical trials talinolol was described to have beneficial effects on triglycerides and cholesterol levels

compared to propranolol.<sup>2–5</sup> These results were investigated in the TALIP study, and it could be shown that talinolol treatment resulted in reduced LDL cholesterol levels in comparison to atenolol.<sup>6</sup> The reduction of the cholesterol levels could not be explained by the inhibition of the beta adrenergic receptors; thus, an off-target activity might be responsible for this pleiotropic effect. These observations make talinolol a valuable starting point for the SOSA approach. However, the optimization of the phenotypic effect is not always rational due to the multifactorial response to a drug.

**Received:** February 26, 2019

**Accepted:** May 29, 2019

**Published:** May 29, 2019

Thus, deorphanization of the target responsible for the side activity makes the optimization procedure straightforward.

Computer-aided target deorphanization, also referred to as polypharmacology detection or target identification, has become popular in the past few years.<sup>7,8</sup> In this study we used three different popular web-based target deorphanization tools to propose alternative targets of talinolol: HitPickV2,<sup>9</sup> SuperPred,<sup>10</sup> and SwissTargetPrediction<sup>11</sup> (see Supporting Information). All three tools independently predicted soluble epoxide hydrolase (sEH) as the most probable novel target of talinolol. Inhibition of sEH is related to cholesterol and lipid lowering effects.<sup>12,13</sup> For propranolol, sEH was absent in the list of the predicted targets produced by all three tools.

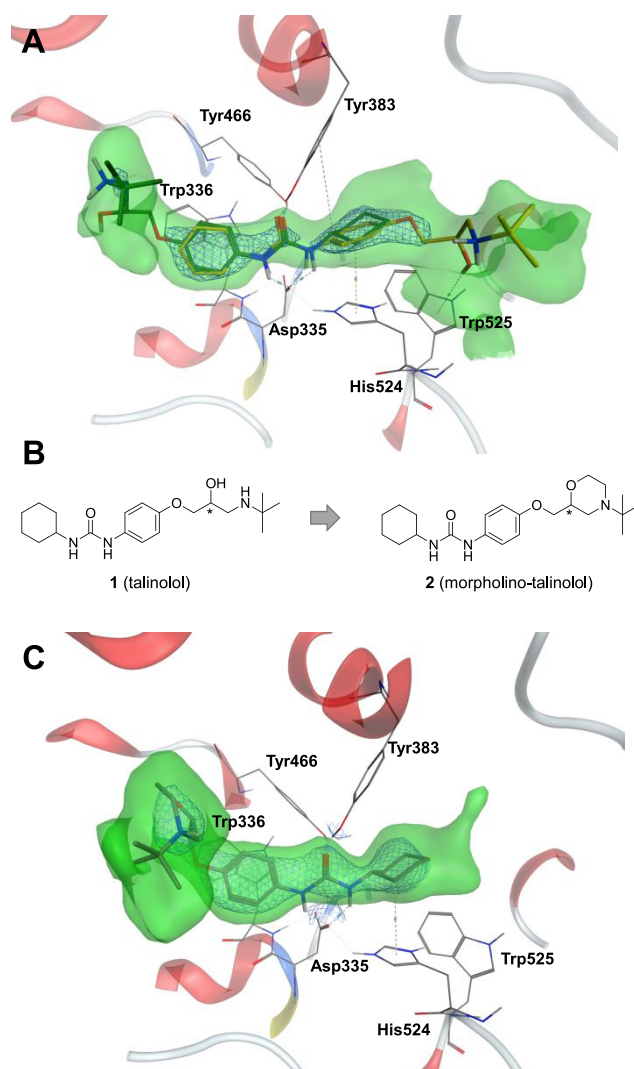
Based on the *in silico* target prediction, we investigated the inhibitory activity of talinolol toward sEH *in vitro* using the fluorogenic substrate PHOME.<sup>14</sup> Talinolol inhibited sEH with an  $IC_{50}$  of 2.8  $\mu$ M, while propranolol remained inactive (Table 1). In human patients, talinolol reaches a  $C_{max}$  of 191 ng/mL

**Table 1. Activity and *in Vitro* Pharmacological Data of Propranolol, Talinolol, and Morpholino-Talinolol**

Property	Propranolol	Talinolol (1)	Morpholino-talinolol (2)
<i>In vitro</i> inhibition of soluble epoxide hydrolase (sEH)	inactive	$IC_{50} = 2.8 \pm 0.2 \mu\text{M}$	$IC_{50} = 0.077 \pm 0.004 \mu\text{M}$
Metabolic stability in RLM after 1 h	$37 \pm 2\%$	$86 \pm 6\%$	$71 \pm 1\%$
Permeability ( $\log P_c$ )	$-1.99 \pm 0.04$	$-5.2 \pm 0.7$	$-2.31 \pm 0.004$

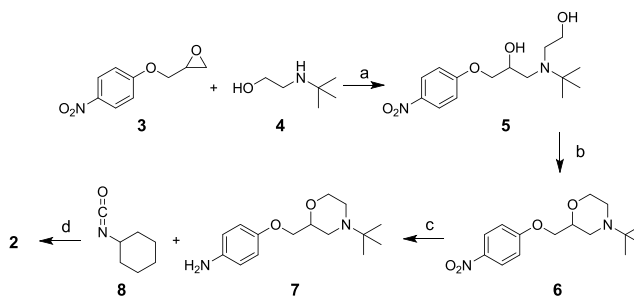
(0.53  $\mu$ M) after 12 weeks application of 100 mg per day.<sup>6</sup> Other studies<sup>2–5</sup> which describe the cholesterol and lipid lowering effects of talinolol were performed with even higher daily dosages of talinolol (200 mg–300 mg) suggesting that these effects could indeed be caused by inhibition of sEH.<sup>16–18</sup> However, although significant results were obtained in this study, the inhibitory potency of talinolol toward sEH is not sufficient for direct repurposing. Furthermore, the blood pressure lowering effects and adverse effects of beta-adrenergic antagonism activity ( $K_i$  ( $\beta$ AR1) = 0.24  $\pm$  0.05  $\mu$ M;  $K_i$  ( $\beta$ AR2) = 0.9  $\pm$  0.1  $\mu$ M) determined by radioligand binding assay of the Psychoactive Drug Screening Program (PDSP)<sup>15</sup> also make the usage of high-dosed talinolol impossible. However, it makes talinolol an ideal candidate for the SOSA approach, which should ideally aim at enhancing the sEH inhibitory activity and simultaneous reduction of the  $\beta$ AR antagonism.

In order to rationalize our SOSA approach, we cocrystallized talinolol with the C-terminal domain of sEH. The binding mode was used for structure-based optimization. We observed two possible orientations of talinolol in the active site of sEH (Figure 1A) with a number of different conformations. The presence of the inhibitor was verified by a polder map shown in green (Figure 1A). The urea moiety substituted by two lipophilic residues was identified as the key pharmacophore responsible for sEH binding, which correlates well with previous studies.<sup>19</sup> The ethanolamine moiety, which is a crucial part of the beta adrenergic receptor pharmacophore, does not form crucial directed interactions with the binding site residues, and the electron density for this moiety is not well-resolved. Thus, we decided to remove the hydrogen



**Figure 1.** Design of morpholino-talinolol. A shows the X-ray crystallographic structure of the C-terminal domain of sEH in complex with talinolol (PDB record 6HGV). Two of the possible conformations of talinolol were modeled in the density of the polder map covering both orientations in the binding pocket. C shows the structure of the C-terminal domain in complex with morpholino-talinolol (PDB record 6HGX). In both structures, the mFo-DFc polder map around the ligand is shown in green (countered at 3 $\sigma$ ), while the 2mFo-DFC map of the ligands is shown in blue (countered at 1 $\sigma$ ). B shows the structure of talinolol (left) and morpholino-talinolol (right).

**Scheme 1. Synthesis of Morpholino-Talinolol.** (a) EtOH,  $\mu$ W, 150  $^{\circ}$ C, 15 bar, 30 min, 20%; (b) 1. NaH, 2. p-TsCl, THF, 0  $^{\circ}$ C – rt, 72 h, 61%; (c) Pd/C, H<sub>2</sub>, EtOH, rt, 6 h, 97%, (d) DIPEA, abs. DCM, rt, 20 h, 33%.



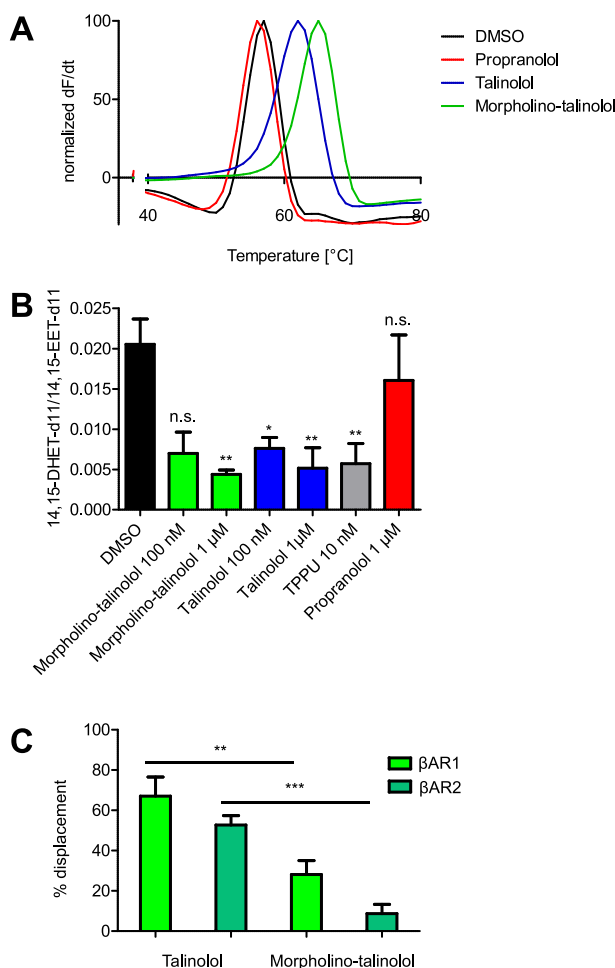


**Figure 2.** (A) Differential scanning fluorimetry assay demonstrates that talinolol and morpholino-talinolol, but not propranolol, stabilize sEH. The graph displays the normalized first derivation of a representative measurement. (B) sEH inhibition in HEP-G2 lysates. ( $\pm$ )14(15)-EET-d11 was used as sEH substrate and the EET/DHET ratios were measured via LC-MS/MS. Results are given as mean + SEM out of three independent experiments. (C) Radioligand displacement of talinolol and morpholino-talinolol from  $\beta$ AR1 and  $\beta$ AR2. The *t* test for B and C for two independent means was performed using a web server (<https://www.socscistatistics.com/tests/studentttest/default2.aspx>, 6th May 2019); \*:  $p < 0.05$ ; \*\*:  $p < 0.01$ ; \*\*\*:  $p < 0.001$ .

bonding functionalities of the ethanolamine moiety by ring closure (Figure 1B). The synthesis of the designed morpholino-talinolol (**2**) was accomplished through coupling of the secondary amine precursor **4** to the epoxide moiety of **3**. Subsequently, ring closure of the morpholine was mediated by *p*-tosyl chloride. The aromatic nitro group of **6** was reduced using palladium on charcoal and coupled to cyclohexyl isocyanate **8** to yield the desired product **2** (see Scheme 1).

Morpholino-talinolol was tested *in vitro*, and significant increase in potency toward sEH could be measured ( $IC_{50} = 0.077 \mu\text{M}$ ). The design hypothesis could be confirmed using X-ray crystallography. The co-crystal structure of morpholino-talinolol and the C-terminal domain of sEH revealed that the urea moiety interacts with the catalytic triad acting as an epoxide mimetic. The cyclohexyl moiety occupies the smaller hydrophobic pocket while the substituted phenyl part reaches into the larger hydrophobic tunnel (see Figure 1C).

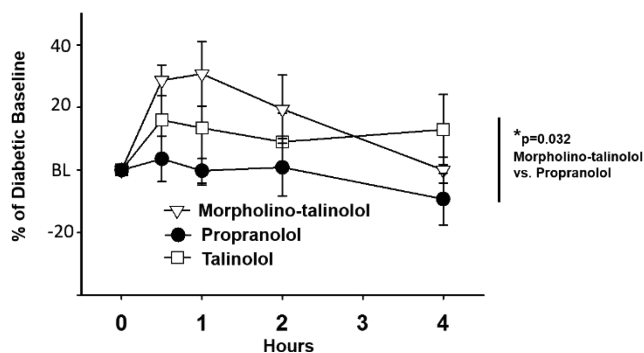


**Figure 3.** Effects of talinolol and derivatives on diabetic neuropathic pain. Pain (allodynia) was assessed in diabetic neuropathic rats ( $n = 6/\text{group}$ ) after single administration of 10 mg/kg each compound in PEG 300. Morpholino-talinolol was significant compared to the effects of propranolol but not talinolol ( $p = 0.032$ ). Two way analysis of variance, Holm-Sidak method post hoc. Naïve baseline averaged 84.6 gr versus diabetic baselines 41.0 gr (normalized above) for all groups.

Morpholino-talinolol displays one dominant orientation in the binding site of sEH.

Differential scanning fluorimetry (DSF) assay was used to confirm the direct binding of morpholino-talinolol to sEH (Figure 2A). Talinolol caused a pronounced shift of the melting point of sEH ( $62.5 \pm 0.5 \text{ }^\circ\text{C}$  vs  $57.0 \pm 0.0 \text{ }^\circ\text{C}$  DMSO control) while propranolol did not affect the temperature-dependent denaturation of sEH significantly ( $56.3 \pm 0.5 \text{ }^\circ\text{C}$ ). Morpholino-talinolol caused a more pronounced thermal shift of  $65.1 \pm 0.3 \text{ }^\circ\text{C}$  which correlates nicely with the lower  $IC_{50}$  value *in vitro*. We could also confirm the sEH inhibitory activity of talinolol and morpholino-talinolol in HEP-G2 cells by monitoring the conversion of 14,15-EET-d11. In this setting, both compounds reduced the conversion of the externally added EET like the most advanced sEH inhibitor TPPU, while propranolol did not show an effect (Figure 2B). As expected from the bridging of the ethanolamine moiety, the binding affinity of morpholino-talinolol toward  $\beta$ ARs was significantly reduced in comparison to talinolol (Figure 2C).

Preliminary evaluation of the *in vitro* metabolic stability and penetrability (Table 1) suggested that morpholino-talinolol should be orally available, which supports the intention of the SOSA approach to deliver lead structures with good initial pharmacokinetics. In order to accomplish the successful SOSA approach, we examined the *in vivo* activity of morpholino-talinolol in comparison to talinolol and propranolol in rats. sEH inhibitors exhibit a pronounced blood pressure lowering effect comparable to beta blockers.<sup>20,21</sup> Furthermore, sEH substrate EETs have pronounced antinociceptive effects, which are strongly enhanced by the application of sEH inhibitors.<sup>22</sup> Therefore, pain was modeled using diabetic neuropathy induced by streptozocin, which targets and kills the pancreatic beta islet cells rendering the rats with type I diabetes and neuropathic pain, in which different sEH inhibitors were found to be active.<sup>23</sup> Propranolol, a beta blocker without sEH inhibitory activity, which was confirmed in three orthogonal assays, was used as negative control in order to exclude the possibility that the antinociceptive effects originate from the  $\beta$ AR antagonism activity. After 5 days the allodynia of diabetic rats was confirmed, and a von Frey assay was performed.<sup>24</sup> Morpholino-talinolol blocked allodynia, and this antinociception was sustained up to 2 h before declining (Figure 3).

This study demonstrates the unique opportunities of *in silico* polypharmacology prediction to deorphanize the side activities of a drug observed in clinical studies. Furthermore, once the target of interest has been discovered, the rational application of the SOSA approach is straightforward. The use of an approved drug warrants an acceptable pharmacokinetic profile while potency optimization can be achieved with a low number of optimization steps.

## ■ ASSOCIATED CONTENT

### ■ Supporting Information

The Supporting Information is available free of charge on the ACS Publications website at DOI: 10.1021/acsmchemlett.9b00075.

Experimental data including synthesis, assay details, crystallization protocol, and animal experiments (PDF)

Target prediction results from HitPickV2, SuperPred, and SwissTargetPrediction (PDF)

## ■ AUTHOR INFORMATION

### Corresponding Author

\*E-mail: [proschak@pharmchem.uni-frankfurt.de](mailto:proschak@pharmchem.uni-frankfurt.de); Phone: +49 69 798 29301.

### ORCID

Bruce D. Hammock: 0000-0003-1408-8317

Ewgenij Proschak: 0000-0003-1961-1859

### Author Contributions

<sup>V</sup>K.H. and J.S.K. contributed equally and are named in alphabetical order. The manuscript was written through contributions of all authors. All authors have given approval to the final version of the manuscript.

### Funding

This research was supported by the German Research Foundation (DFG; PR1405/2-2, PR1405/4-1, SFB1039 Teilprojekt A02, and Teilprojekt A07) and National Institute of Environmental Health Sciences (NIEHS) Grant R01 ES002710 and NIEHS Superfund Research Program P42 ES004699. K.H. was supported by the Else-Kroener-Fresenius-Foundation funding the graduate school 'Translational Research Innovation – Pharma' (TRIP).

### Notes

The authors declare no competing financial interest.

## ■ ACKNOWLEDGMENTS

The crystal diffraction experiments were performed on beamline ID-29 at the European Synchrotron Radiation Facility (ESRF), Grenoble, France. We thank the staff of ESRF for assistance and support in using beamline ID-29. Ki determinations were generously provided by the National Institute of Mental Health's Psychoactive Drug Screening Program, Contract # HHSN-271-2018-00023-C (NIMH PDSP). The NIMH PDSP is directed by Bryan L. Roth MD, PhD, at the University of North Carolina at Chapel Hill and Project Officer Jamie Driscoll at NIMH, Bethesda MD, USA.

## ■ ABBREVIATIONS

LDL, low density lipoprotein; PDSP, Psychoactive Drug Screening Program; sEH, soluble epoxide hydrolase; SOSA, selective optimization of side activities

## ■ REFERENCES

- (1) Wermuth, C. G. Selective Optimization of Side Activities: The SOSA Approach. *Drug Discovery Today* **2006**, *11* (3–4), 160–164.
- (2) Gräfer, L.; Seidel, B. Prazosin, Talinolol Und Cholesterolemabismus - Wirkt Talinolol Auch Potentiell Atherogen? *Nieren-Hochdruckkrkh* **1991**, *20*, 176–181.
- (3) Hanefeld, M.; Weigmann, I.; Julius, U.; May, C.; Schwanebeck, U.; Terhaag, B. Vergleichende Untersuchungen Zum Einfluß Der  $\beta$ -Blocker Talinolol Und Metoprolol Auf Den Lipid- Und Kohlenhydratstoffwechsel Bei Typ-II-Diabetes. *Diabetes Stoffwechsel* **1999**, *8*, 1–6.
- (4) Homuth, V.; Pahl, L. Langzeittherapie von Frühstadien Der Arteriellen Hypertonie Mit Dem Selektiven Adrenergen  $\beta$ 1-Rezeptorenblocker Talinolol (Cordanum) In Verbindung Mit Fahrradergometrischen Und Echokardiographischen Untersuchungen. *Dtsch Gesundheitsw* **1981**, *36*, 1294–1299.
- (5) Schauer, I.; Schauer, U. Nebenwirkungen von Propranolol Und Talinolol Auf Den Plasmalipidstoffwechsel. *Dtsch Gesundheitsw* **1984**, *39*, 706–709.
- (6) Sourgens, H.; Schmidt, J.; Derendorf, H. Comparison of Talinolol and Atenolol Effects on Blood Pressure in Relation to Lipid and Glucose Metabolic Parameters. Results from the TALIP Study. *Int. J. Clin Pharmacol Ther* **2003**, *41* (1), 22–29.
- (7) Lavecchia, A.; Cerchia, C. In Silico Methods to Address Polypharmacology: Current Status, Applications and Future Perspectives. *Drug Discovery Today* **2016**, *21* (2), 288–298.
- (8) Achenbach, J.; Tiikkainen, P.; Franke, L.; Proschak, E. Computational Tools for Polypharmacology and Repurposing. *Future Med. Chem.* **2011**, *3* (8), 961–968.
- (9) Hamad, S.; Adornetto, G.; Naveja, J.; Ravindranath, A. C.; Raffler, J.; Campillos, M. HitPickV2: A Web Server to Predict Targets of Chemical Compounds. *Bioinformatics* **2019**, *35*, 1239.
- (10) Nickel, J.; Gohlke, B.-O.; Erehman, J.; Banerjee, P.; Rong, W. W.; Goede, A.; Dunkel, M.; Preissner, R. SuperPred: Update on Drug Classification and Target Prediction. *Nucleic Acids Res.* **2014**, *42* (Web Server issue), W26–31.
- (11) Gfeller, D.; Grosdidier, A.; Wirth, M.; Daina, A.; Michielin, O.; Zoete, V. SwissTargetPrediction: A Web Server for Target Prediction of Bioactive Small Molecules. *Nucleic Acids Res.* **2014**, *42* (Web Server issue), W32–38.
- (12) Mangels, N.; Awwad, K.; Wettenmann, A.; Dos Santos, L. R. B.; Frömel, T.; Fleming, I. The Soluble Epoxide Hydrolase Determines Cholesterol Homeostasis by Regulating AMPK and SREBP Activity. *Prostaglandins Other Lipid Mediators* **2016**, *125*, 30–39.
- (13) Roche, C.; Besnier, M.; Cassel, R.; Harouki, N.; Coquerel, D.; Guerrot, D.; Nicol, L.; Loizon, E.; Remy-Jouet, I.; Morisseau, C.; et al. Soluble Epoxide Hydrolase Inhibition Improves Coronary Endothelial Function and Prevents the Development of Cardiac Alterations in Obese Insulin-Resistant Mice. *Am. J. Physiol. Heart Circ. Physiol.* **2015**, *308* (9), H1020–1029.
- (14) Wolf, N. M.; Morisseau, C.; Jones, P. D.; Hock, B.; Hammock, B. D. Development of a High-Throughput Screen for Soluble Epoxide Hydrolase Inhibition. *Anal. Biochem.* **2006**, *355* (1), 71–80.
- (15) Besnard, J.; Ruda, G. F.; Setola, V.; Abecassis, K.; Rodriguiz, R. M.; Huang, X.-P.; Norval, S.; Sassano, M. F.; Shin, A. I.; Webster, L. A.; et al. Automated Design of Ligands to Polypharmacological Profiles. *Nature* **2012**, *492* (7428), 215–220.
- (16) Mangels, N.; Awwad, K.; Wettenmann, A.; Dos Santos, L. R. B.; Frömel, T.; Fleming, I. The Soluble Epoxide Hydrolase Determines Cholesterol Homeostasis by Regulating AMPK and SREBP Activity. *Prostaglandins Other Lipid Mediators* **2016**, *125*, 30–39.
- (17) Roche, C.; Besnier, M.; Cassel, R.; Harouki, N.; Coquerel, D.; Guerrot, D.; Nicol, L.; Loizon, E.; Remy-Jouet, I.; Morisseau, C.; et al. Soluble Epoxide Hydrolase Inhibition Improves Coronary Endothelial Function and Prevents the Development of Cardiac Alterations in Obese Insulin-Resistant Mice. *Am. J. Physiol. Heart Circ. Physiol.* **2015**, *308* (9), H1020–1029.
- (18) Shen, L.; Peng, H.; Peng, R.; Fan, Q.; Zhao, S.; Xu, D.; Morisseau, C.; Chiamvimonvat, N.; Hammock, B. D. Inhibition of

Soluble Epoxide Hydrolase in Mice Promotes Reverse Cholesterol Transport and Regression of Atherosclerosis. *Atherosclerosis* **2015**, *239* (2), 557–565.

(19) Huang, S.-X.; Li, H.-Y.; Liu, J.-Y.; Morisseau, C.; Hammock, B. D.; Long, Y.-Q. Incorporation of Piperazino Functionality into 1,3-Disubstituted Urea as the Tertiary Pharmacophore Affording Potent Inhibitors of Soluble Epoxide Hydrolase with Improved Pharmacokinetic Properties. *J. Med. Chem.* **2010**, *53* (23), 8376–8386.

(20) Imig, J. D.; Walsh, K. A.; Hye Khan, M. A.; Nagasawa, T.; Cherian-Shaw, M.; Shaw, S. M.; Hammock, B. D. Soluble Epoxide Hydrolase Inhibition and Peroxisome Proliferator Activated Receptor  $\gamma$  Agonist Improve Vascular Function and Decrease Renal Injury in Hypertensive Obese Rats. *Exp. Biol. Med. (London, U. K.)* **2012**, *237* (12), 1402–1412.

(21) Hye Khan, M. A.; Kolb, L.; Skibba, M.; Hartmann, M.; Blöcher, R.; Proschak, E.; Imig, J. D. A Novel Dual PPAR- $\gamma$  Agonist/SEH Inhibitor Treats Diabetic Complications in a Rat Model of Type 2 Diabetes. *Diabetologia* **2018**, *61* (10), 2235–2246.

(22) Wagner, K. M.; McReynolds, C. B.; Schmidt, W. K.; Hammock, B. D. Soluble Epoxide Hydrolase as a Therapeutic Target for Pain, Inflammatory and Neurodegenerative Diseases. *Pharmacol. Ther.* **2017**, *180*, 62–76.

(23) Lee, K. S. S.; Liu, J.-Y.; Wagner, K. M.; Pakhomova, S.; Dong, H.; Morisseau, C.; Fu, S. H.; Yang, J.; Wang, P.; Ulu, A.; et al. Optimized Inhibitors of Soluble Epoxide Hydrolase Improve in Vitro Target Residence Time and in Vivo Efficacy. *J. Med. Chem.* **2014**, *57* (16), 7016–7030.

(24) Wagner, K.; Inceoglu, B.; Dong, H.; Yang, J.; Hwang, S. H.; Jones, P.; Morisseau, C.; Hammock, B. D. Comparative Efficacy of 3 Soluble Epoxide Hydrolase Inhibitors in Rat Neuropathic and Inflammatory Pain Models. *Eur. J. Pharmacol.* **2013**, *700* (1–3), 93–101.